Sufficient Conditions for the Suboptimality of Identical Quantizer Distributed Detection

Chun-Yen Yang

Institute of Communications Engineering,
National Chiao Tung University,
Hsin Chu, Taiwan 30050, R.O.C.

July 4, 2013

Outline

- Introduction
- Preliminaries
- The Best Quantizers for Finite Number of Sensors
- Regions that the Identical Quantizer System (IQS) is Suboptimal
- Simulation Results
- Conclusion and Future Work

Introduction

Introduction

- Consider a distributed detection system consisting of n sensors and a fusion center.
- The ith sensor receives an observation Y_i.
- Y_i is quantized into an m-ary data $U_i = f(Y_i)$, which is then sent to the fusion center.
- Based on the received data $(U_1, \ldots, U_n)$, the future center determines which of the two hypotheses, H_0 or H_1, is the true one.

Introduction

- In its practice, it is more engineeringly convenient to quantize each Y_i by the same quantization rule, named *identical quantizer system* (IQS).
- However, it is known that such an identical quantizer system design is sometimes only suboptimal in detection error.
- We denote the detection error of the optimal (possibly non-identical) distributed detection system by $\gamma^*(\pi)$, and use $\gamma^\diamond(\pi)$ to denote the detection error of the best identical quantizer system.
- π is the prior probability of the null hypothesis H_0.
- In this thesis, we will study what distribution of local observation Y_i will give

$$\gamma^*(\pi) < \gamma^\diamond(\pi)$$

for finite n.
- Specifically, we investigate when changing one local quantizer to a distinct one can yields a better performance than the IQS.

Preliminaries

System Setting

In our setting, the two hypotheses are assumed equally likely.

For simplicity, we assume ternary local observation space and binary quantization.

The statistics for local observations in $\{a_1, a_2, a_3\}$ is denoted parametrically by:

y	a_1	a_2	a_3
$\Pr(y\|H_0)$	P_1	P_2	$1 - P_1 - P_2$
$\Pr(y\|H_1)$	$1 - Q_1 - Q_2$	Q_1	Q_2

System Setting

Based on the above setting, there are only two nontrivial deterministic likelihood ratio quantizers (LRQs) if either

$$\frac{\Pr(a_1|H_1)}{\Pr(a_1|H_0)} \geq \frac{\Pr(a_2|H_1)}{\Pr(a_2|H_0)} \geq \frac{\Pr(a_3|H_1)}{\Pr(a_3|H_0)} \tag{1}$$

or

$$\frac{\Pr(a_1|H_1)}{\Pr(a_1|H_0)} \leq \frac{\Pr(a_2|H_1)}{\Pr(a_2|H_0)} \leq \frac{\Pr(a_3|H_1)}{\Pr(a_3|H_0)} \tag{2}$$

These two LRQs are

- $\hat{g}$ (which partitions local observation space $\{a_1, a_2, a_3\}$ to $\{a_1\}$ and $\{a_2, a_3\}$),
- and $\bar{g}$ (which partitions local observation space $\{a_1, a_2, a_3\}$ to $\{a_1, a_2\}$ and $\{a_3\}$).

Because the local observations $Y_1, \ldots, Y_n$ are i.i.d., each local sensor in the optimal system should adopt either $\hat{g}$ or $\bar{g}$ as the local quantizer.

Table:

u	0	1
$P_{\hat{g}}(u) = \Pr(u\|H_0)$	P_1	$1 - P_1$
$Q_{\hat{g}}(u) = \Pr(u\|H_1)$	$1 - Q_1 - Q_2$	$Q_1 + Q_2$
u	0	1
$P_{\bar{g}}(u) = \Pr(u\|H_0)$	$P_1 + P_2$	$1 - P_1 - P_2$
$Q_{\bar{g}}(u) = \Pr(u\|H_1)$	$1 - Q_2$	Q_2

Background and Distribution Detection

Here we will provide an example from the followup work we cite. The two hypothesis distributions are specified as indicated below.

Y	a_1	a_2	a_3
$P(y) = \Pr(y\|H_0)$	$1/12$	$1/4$	$2/3$
$Q(y) = \Pr(y\|H_1)$	$1/3$	$1/3$	$1/3$
$(dP/dQ)(y)$	$1/4$	$3/4$	2

Under this setting, there are only two nontrivial deterministic LRQ's, as having been stated previously. Their post-quantization distributions are listed in this table.

Table:

u	0	1
$P_{\hat{g}}(u)$	1/12	11/12
$Q_{\hat{g}}(u)$	1/3	2/3
u	0	1
$P_{\bar{g}}(u)$	1/3	2/3
$Q_{\bar{g}}(u)$	2/3	1/3

We then derive:

$$\gamma_n\left(\frac{1}{2}\right) = \sum_{l=0}^{n-1}\binom{n-1}{l}\left(\frac{2^l+2^{n-l-1}}{2\cdot 3^{n-1}}\right)\cdot\gamma_1\left(\frac{2^{2l-n+1}}{2^{2l-n+1}+1}\right). \tag{3}$$

where $\gamma_1(\cdot)$ is the Bayes detection error for a system with only one sensor, and we use for notational convenience $(x \wedge y)$ to denote $\min\{x, y\}$.

$$\gamma_n\left(\frac{1}{2}\right) = \sum_{l=0}^{n-1}\binom{n-1}{l}\left(\frac{2^l+2^{n-l-1}}{2\cdot 3^{n-1}}\right)\cdot\gamma_1\left(\frac{2^{2l-n+1}}{2^{2l-n+1}+1}\right). \tag{3}$$

The last output u_n can be resulted from either local quantization rule $\hat{g}$ or $\bar{g}$. Accordingly, γ_1 can have two different formulas, which are respectively denoted by $\hat{\gamma}_1$ and $\bar{\gamma}_1$ for quantization rules $\hat{g}$ and $\bar{g}$. Their formulas are:

$$\hat{\gamma}_1(\pi) = \left(\frac{1}{12}\pi \wedge \frac{1}{3}(1-\pi)\right) + \left(\frac{11}{12}\pi \wedge \frac{2}{3}(1-\pi)\right)$$

and

$$\bar{\gamma}_1(\pi) = \left(\frac{1}{3}\pi \wedge \frac{2}{3}(1-\pi)\right) + \left(\frac{2}{3}\pi \wedge \frac{1}{3}(1-\pi)\right),$$

Note that $\hat{\gamma}_1(\pi) = \bar{\gamma}_1(\pi)$ for $0 \leq \pi \leq 1/3$, $\pi = 4/7$ and $4/5 \leq \pi \leq 1$. Thus the critical values of l are those for which $2^{2l-n+1}/(2^{2l-n+1}+1)$ lies in the union of $(1/3, 4/7)$ and $(4/7, 4/5)$.

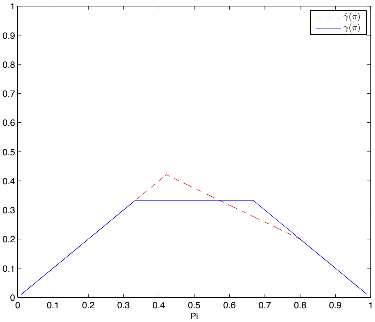

Figure: Functions of $\hat{\gamma}_1(\pi)$ and $\bar{\gamma}_1(\pi)$, where $\hat{\gamma}_1(\pi)$ is plotted in solid blue color, while $\bar{\gamma}_1(\pi)$ in dotted red color.

Equivalently, the critical l's lies in

$$\frac{n-2}{2} < l < \frac{n+1-\log_2(3)}{2} \approx \frac{n-0.585}{2} \quad \text{and} \quad \frac{n+1-\log_2(3)}{2} < l < \frac{n+1}{2}.$$

When $n = 2k$ is even,

$$k-1 < l < \frac{2k+1-\log_2(3)}{2} \approx k - 0.292 \quad \text{and} \quad k - 0.292 < l < k + 0.5.$$

So the only critical value of l is $n/2 = k$, which implies that

$$\frac{2^{2l-n+1}}{2^{2l-n+1}+1} = \frac{2}{3}.$$

Since $\hat{\gamma}(2/3) = 5/18 < 1/3 = \bar{\gamma}(2/3)$, there exists a *non-identical quantizer system* performed better than the best identical quantizer system. Hence, the optimal system must be a non-identical quantizer system.

$$\gamma_n\left(\frac{1}{2}\right) = \sum_{l=0}^{n-1} \binom{n-1}{l} \left(\frac{2^l + 2^{n-l-1}}{2 \cdot 3^{n-1}}\right) \cdot \gamma_1\left(\frac{2^{2l-n+1}}{2^{2l-n+1}+1}\right). \tag{3}$$

The Best Quantizers for Finite Number of Sensors

We examine the specific case that the alternative hypothesis distribution is uniform. The statistics for local observations $\{a_1, a_2, a_3\}$ can be given as follows.

y	a_1	a_2	a_3
$\Pr(y\|H_0)$	P_1	P_2	$1 - P_1 - P_2$
$\Pr(y\|H_1)$	$\frac{1}{3}$	$\frac{1}{3}$	$\frac{1}{3}$

We then increase P_1 and P_2 from 0 to 1 under $P_1 + P_2 < 1$. During this process, we fix the number of sensors n. Our experimental results indicate which IQS (among type-1 IQS, type-2 IQS, and type-3 IQS; see the table in the next slide) should be used can be clearly characterized into six regions.

Table: The condition on P_1 and P_2 specified below is the range in which the respective post-quantization LRQ is of effectively use in detection.

(a) $P_1 > \max\{P_2, (1-P_2)/2\}$ or $P_1 < \min\{P_2, (1-P_2)/2\}$

u	$0 \equiv \{a_1\}$	$1 \equiv \{a_2, a_3\}$
$P_{g_1}(u)$	P_1	$1-P_1$
$Q_{g_1}(u)$	$\frac{1}{3}$	$\frac{2}{3}$

(b) $\min\{P_2, 1-2P_2\} < P_1 < \max\{P_2, 1-2P_2\}$

u	$0 \equiv \{a_2\}$	$1 \equiv \{a_1, a_3\}$
$P_{g_2}(u)$	P_2	$1-P_2$
$Q_{g_2}(u)$	$\frac{1}{3}$	$\frac{2}{3}$

(c) $P_1 < \min\{(1-P_2)/2, 1-2P_2\}$ or $P_1 > \max\{(1-P_2)/2, 1-2P_2\}$

u	$0 \equiv \{a_1, a_2\}$	$1 \equiv \{a_3\}$
$P_{g_3}(u)$	P_1+P_2	$1-P_1-P_2$
$Q_{g_3}(u)$	$\frac{2}{3}$	$\frac{1}{3}$

By denoting the error probabilities of the IQS for type 1, type 2 and type 3 local quantizers respectively by $\gamma_{n,1}$, $\gamma_{n,2}$ and $\gamma_{n,3}$, we derive for different P_1 and P_2 as follows:

$$\begin{aligned} & \gamma_{n,1}\left(\frac{1}{2}\right) \\ = \quad & \frac{1}{2}\sum_{l=0}^{n-1}\binom{n-1}{l}\left\{\left[P_1^{l+1}(1-P_1)^{n-1-l}\wedge(\frac{1}{3})^{l+1}(\frac{2}{3})^{n-1-l}\right]+\left[P_1^{l}(1-P_1)^{n-l}\wedge(\frac{1}{3})^{l}(\frac{2}{3})^{n-l}\right]\right\} \end{aligned} \tag{4}$$

$$\begin{aligned}
&\gamma_{n,2}\left(\frac{1}{2}\right) \\
= \quad & \frac{1}{2}\sum_{l=0}^{n-1}\binom{n-1}{l}\left\{\left[P_2^{l+1}(1-P_2)^{n-1-l}\wedge(\frac{1}{3})^{l+1}(\frac{2}{3})^{n-1-l}\right]+\left[P_2^{l}(1-P_2)^{n-l}\wedge(\frac{1}{3})^{l}(\frac{2}{3})^{n-l}\right]\right\}
\end{aligned} \tag{5}$$

$$\begin{aligned}
&\gamma_{n,3}\left(\frac{1}{2}\right) \\
= \quad & \frac{1}{2}\sum_{l=0}^{n-1}\binom{n-1}{l}\left\{\left[P_3^{l+1}(1-P_3)^{n-1-l}\wedge(\frac{2}{3})^{l+1}(\frac{1}{3})^{n-1-l}\right]+\left[P_3^{l}(1-P_3)^{n-l}\wedge(\frac{2}{3})^{l}(\frac{1}{3})^{n-l}\right]\right\}
\end{aligned} \tag{6}$$

where for convenience, we let $P_3 = 1 - P_1 - P_2$.

With the availability of these error formulas, the boundaries of the six regions can be characterized by the following six formulas:

$$\begin{array}{l}
\gamma_{n,1}\left(\frac{1}{2}\right) = \gamma_{n,2}\left(\frac{1}{2}\right) \text{ for } 0 < P_1 < \frac{1}{3} \text{ and } \frac{1}{3} < P_2 < 1 \\
\gamma_{n,1}\left(\frac{1}{2}\right) = \gamma_{n,2}\left(\frac{1}{2}\right) \text{ for } \frac{1}{3} < P_1 < 1 \text{ and } 0 < P_2 < \frac{1}{3} \\
\gamma_{n,1}\left(\frac{1}{2}\right) = \gamma_{n,3}\left(\frac{1}{2}\right) \text{ for } \frac{1}{3} < P_1 < 1 \text{ and } 0 < P_2 < \frac{1}{3} \\
\gamma_{n,1}\left(\frac{1}{2}\right) = \gamma_{n,3}\left(\frac{1}{2}\right) \text{ for } 0 < P_1 < \frac{1}{3} \text{ and } 0 < P_2 < \frac{1}{3} \\
\gamma_{n,2}\left(\frac{1}{2}\right) = \gamma_{n,3}\left(\frac{1}{2}\right) \text{ for } 0 < P_1 < \frac{1}{3} \text{ and } 0 < P_2 < \frac{1}{3} \\
\gamma_{n,2}\left(\frac{1}{2}\right) = \gamma_{n,3}\left(\frac{1}{2}\right) \text{ for } 0 < P_1 < \frac{1}{3} \text{ and } \frac{1}{3} < P_2 < 1
\end{array}$$

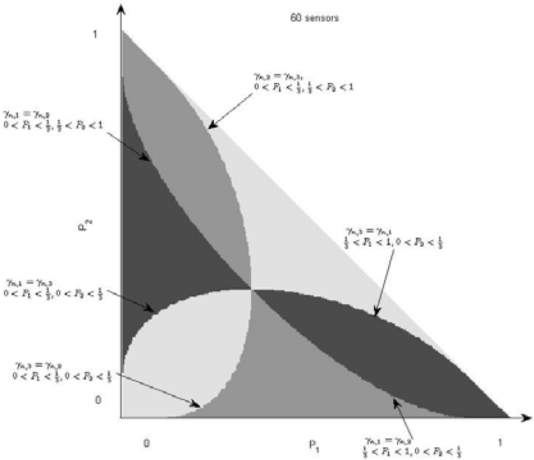

Figure: Regions of the best IQSs. The dark-gray, gray and light-gray areas respectively correspond to the regions that $\gamma_{n,1}$, $\gamma_{n,2}$, and $\gamma_{n,3}$ are the best IQSs.

Regions that the IQS is Suboptimal

After identifying the best IQS for a given hypothesis distribution, we next test whether the NQS can improve the best IQS or not.

As aforementioned, to disprove the optimality of the IQS, we choose to replace one of the sensors' LRQ by a distinct one.

By following similar technique, we prove that in the below regions, the best IQS is only suboptimal.

$$\begin{aligned}
&\text{Segment 1: } (n-1) \text{ type } 1 + 1 \text{ type } 2 : P_1 = \tfrac{2}{3}, \tfrac{5}{64} \le P_2 < \tfrac{1}{6} \\
&\text{Segment 2: } (n-1) \text{ type } 1 + 1 \text{ type } 3 : P_1 = \tfrac{2}{3}, \tfrac{1}{6} < P_2 \le \tfrac{49}{192} \\
&\text{Segment 3: } (n-1) \text{ type } 2 + 1 \text{ type } 1 : P_2 = \tfrac{2}{3}, \tfrac{5}{64} \le P_1 < \tfrac{1}{6} \\
&\text{Segment 4: } (n-1) \text{ type } 2 + 1 \text{ type } 3 : P_2 = \tfrac{2}{3}, \tfrac{1}{6} < P_1 \le \tfrac{49}{192} \\
&\text{Segment 5: } (n-1) \text{ type } 3 + 1 \text{ type } 1 : P_1 + P_2 = \tfrac{3}{4}, \tfrac{21}{64} \le P_1 < \tfrac{3}{8}, \tfrac{3}{8} < P_2 \le \tfrac{27}{64} \\
&\text{Segment 6: } (n-1) \text{ type } 3 + 1 \text{ type } 2 : P_1 + P_2 = \tfrac{3}{4}, \tfrac{3}{8} < P_1 \le \tfrac{27}{64}, \tfrac{21}{64} \le P_2 < \tfrac{3}{8}
\end{aligned} \tag{7}$$

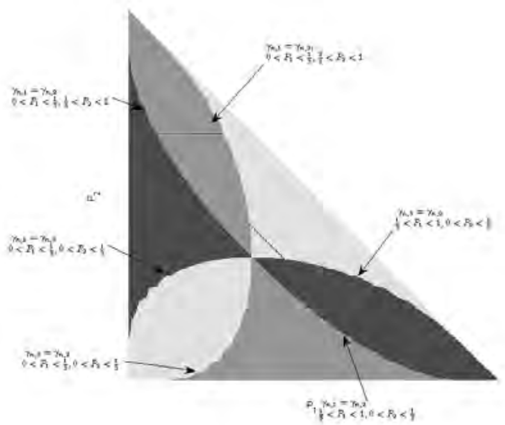

Figure: Regions of the best IQSs. The dark-gray, gray and light-gray areas respectively correspond to the regions that $\gamma_{n,1}$, $\gamma_{n,2}$, and $\gamma_{n,3}$ are the best IQSs. In addition, the line sections of colors dark red, light red, dark green, light green, dark blue and light blue correspond to Segments 1, 2, 3, 4, 5 and 6.

Now take the first segment as an example. We have already known that the type-1 IQS is the best IQS in the specified ranges of P_1 and P_2. We then replace one of the local quantizer to a type-2 quantizer $\hat{g}$. For reader's convenience, the post-quantization hypothesis distributions of the type-1 and type-2 quantizers are tabulated as follows.

Table:

u	0	1
$P_{\bar{g}}(u)$	P_1	$1 - P_1$
$P_{\bar{g}}(u)$	$\frac{1}{3}$	$\frac{2}{3}$
u	0	1
$P_{\hat{g}}(u)$	P_2	$1 - P_2$
$Q_{\hat{g}}(u)$	$\frac{1}{3}$	$\frac{2}{3}$

We now give a detailed derivation for line segment 1. For $P_1 = 2/3$, the two gamma functions are given by:

$$
\begin{aligned}
\bar{r}(\pi) &= \left[P_1\pi \ \wedge\ \frac{1}{3}(1-\pi)\right] + \left[(1-P_1)\pi \ \wedge\ \frac{2}{3}(1-\pi)\right] \\
&= \left[\frac{2}{3}\pi \ \wedge\ \frac{1}{3}(1-\pi)\right] + \left[\frac{1}{3}\pi \ \wedge\ \frac{2}{3}(1-\pi)\right] \\
&= \begin{cases} \frac{2}{3}\pi + \frac{1}{3}\pi, & 0 \le \pi < \frac{1}{3} \\ \frac{1}{3}(1-\pi) + \frac{1}{3}\pi, & \frac{1}{3} \le \pi < \frac{2}{3} \\ \frac{1}{3}(1-\pi) + \frac{2}{3}(1-\pi), & \frac{2}{3} \le \pi \le 1 \end{cases} \\
&= \begin{cases} \pi, & 0 \le \pi < \frac{1}{3} \\ \frac{1}{3}, & \frac{1}{3} \le \pi < \frac{2}{3} \\ 1-\pi, & \frac{2}{3} \le \pi \le 1 \end{cases}
\end{aligned}
$$

and for $P_2 < 1 - P_1 = 1/3$,

$$
\begin{aligned}
\hat{r}(\pi) &= \left[P_2\pi \ \wedge \ \frac{1}{3}(1-\pi)\right] + \left[(1-P_2)\pi \ \wedge \ \frac{2}{3}(1-\pi)\right] \\
&= \begin{cases} P_2\pi + (1-P_2)\pi, & 0 \le \pi < \frac{2}{5-3P_2} \\ P_2\pi + \frac{2}{3}(1-\pi), & \frac{2}{5-3P_2} \le \pi < \frac{1}{3P_2+1} \\ \frac{1}{3}(1-\pi) + \frac{2}{3}(1-\pi), & \frac{1}{3P_2+1} \le \pi \le 1 \end{cases} \\
&= \begin{cases} \pi, & 0 \le \pi < \frac{2}{5-3P_2} \\ P_2\pi + \frac{2}{3}(1-\pi), & \frac{2}{5-3P_2} \le \pi < \frac{1}{3P_2+1} \\ 1-\pi, & \frac{1}{3P_2+1} \le \pi \le 1 \end{cases}
\end{aligned}
$$

The two ranges that $\hat{\gamma}(\pi) \neq \bar{\gamma}(\pi)$ are $(\frac{1}{3}, \frac{1}{2-3P_2})$ and $(\frac{1}{2-3P_2}, \frac{1}{3P_2+1})$, where $\hat{\gamma}(\pi)$ is larger than $\bar{\gamma}(\pi)$ in the former range but is smaller than $\bar{\gamma}(\pi)$ in the latter range. This results in the derivation that

$$\frac{1}{3} < \frac{1}{1+2^{n-1-2l}} < \frac{1}{2-3P_2} \quad \text{and} \quad \frac{1}{2-3P_2} < \frac{1}{1+2^{n-1-2l}} < \frac{1}{3P_2+1},$$

or equivalently,

$$\frac{n}{2} - 1 < l < \frac{n}{2} - \frac{1}{2} - \frac{1}{2}\log_2(1-3P_2) \tag{8}$$

and

$$\frac{n}{2} - \frac{1}{2} - \frac{1}{2}\log_2(1-3P_2) < l < \frac{n}{2} - \frac{1}{2} - \frac{1}{2}\log_2(3P_2). \tag{9}$$

Suppose $n = 2k$ is even. Therefore, if

$$k - \frac{1}{2} - \frac{1}{2}\log_2(1-3P_2) < k \quad \text{(i.e., } P_2 < \frac{1}{6}\text{)},$$

then no integer l satisfies (8).

Note that $P_2 < \frac{1}{6}$ implies that $-\frac{1}{2} - \frac{1}{2}\log_2(1-3P_2) < 0$, and $-\frac{1}{2} - \frac{1}{2}\log_2(3P_2) > 0$.

We conclude that when $P_1 = \frac{2}{3}$ and $0 \le P_2 < \frac{1}{6}$, using $(n-1)$ type 1 + 1 type 2 quantizers always outperform $\gamma_{n,1}$.

Since Figure 2 indicates that $\gamma_{n,1}$ is the optimal IQS between the two margins of $\gamma_{n,1} = \gamma_{n,2}$ and $\gamma_{n,1} = \gamma_{n,3}$ for $\frac{1}{3} \le P_1 \le 1$ and $0 \le P_2 \le \frac{1}{3}$, we can then decide numerically that for the line segment decided by $P_1 = \frac{2}{3}$ and $\frac{5}{64} \le P_2 < \frac{1}{6}$, the IQS is only suboptimal.

The proofs for the other five line segments are similar; hence, we omit them.

Simulation Results (that motivates our research)

What presented in the following figures is the performances of the hypothesis setting below.

y	a_1	a_2	a_3
$\Pr(y\|H_0)$	1/12	1/4	2/3
$\Pr(y\|H_1)$	1/3	1/3	1/3

After binary quantization, it will result in two nontrivial LRQs as shown in the table below.

Table:

u	0	1
$P_{\hat{g}}(u) = \Pr(u\|H_0)$	1/12	1/12
$Q_{\hat{g}}(u) = \Pr(u\|H_1)$	1/3	2/3

u	0	1
$P_{\bar{g}}(u) = \Pr(u\|H_0)$	1/3	2/3
$Q_{\bar{g}}(u) = \Pr(u\|H_1)$	2/3	1/3

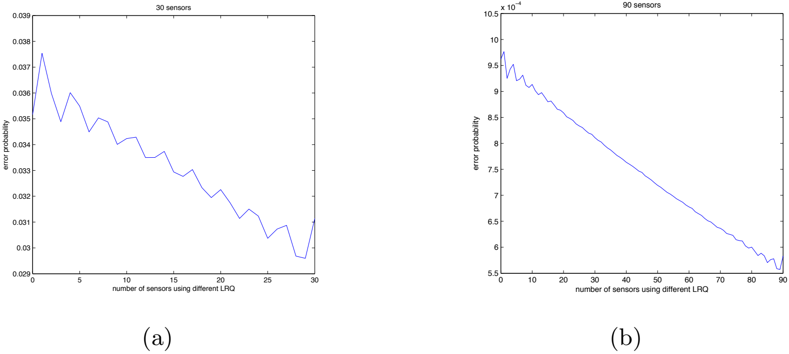

Figure: Detect errors for the LRQs in table at page 33. The x-axis indicates the number of sensors that use LRQ $\hat{g}$. As indicated on top of the plots, the total numbers of sensors are respectively 30 and 90 in (a) and (b).

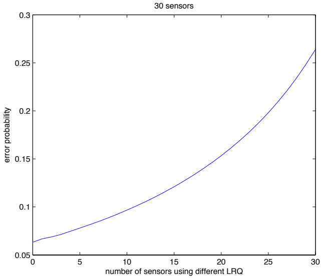

(a)

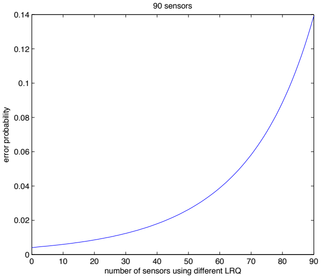

(b)

Figure: Detect errors for the LRQs by another case. The x-axis indicates the number of sensors that use LRQ $\hat{g}$. As indicated on top of the plots, the total numbers of sensors are respectively 30 and 90 in (a) and (b).

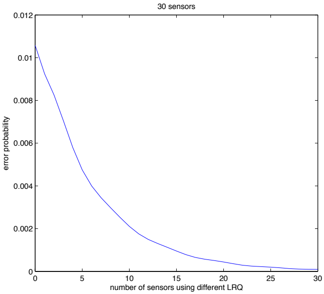

(a)

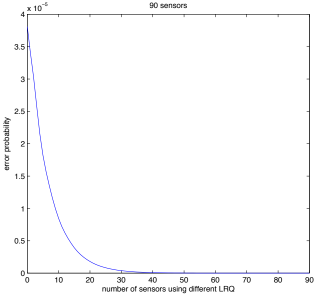

(b)

Figure: Detect errors for the LRQs by another case. The x-axis indicates the number of sensors that use LRQ $\hat{g}$. As indicated on top of the plots, the total numbers of sensors are respectively 30 and 90 in (a) and (b).

The following figures show the areas, in which the NQS with one different local LRQ improves the best IQS. When such an improvement occurs, we will use the following colors to indicate it:

$$\begin{aligned}
&(n-1)\text{ type }1+1\text{ type }2:\text{dark red}\\
&(n-1)\text{ type }1+1\text{ type }3:\text{red}\\
&(n-1)\text{ type }2+1\text{ type }1:\text{dark green}\\
&(n-1)\text{ type }2+1\text{ type }3:\text{green}\\
&(n-1)\text{ type }3+1\text{ type }1:\text{dark blue}\\
&(n-1)\text{ type }3+1\text{ type }2:\text{blue}
\end{aligned} \tag{10}$$

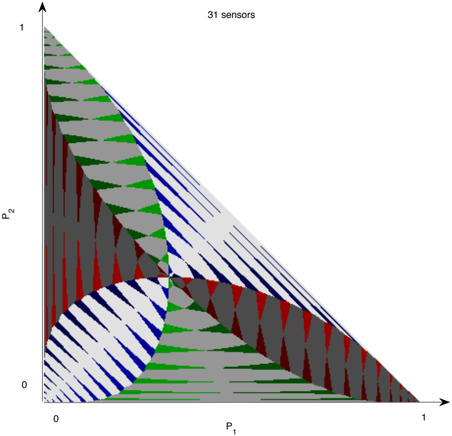

Figure: Areas that the NQS with one different LRQ outperforms the best IQS. The implications of different colors are designated in (10). The number of sensors is 31.

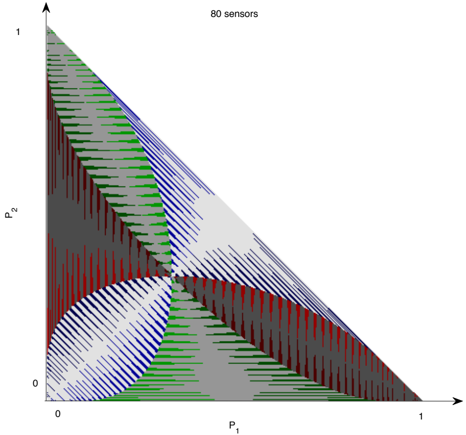

Figure: Areas that the NQS with one different LRQ outperforms the best IQS. The implications of different colors are designated in (10). The number of sensors is 80.

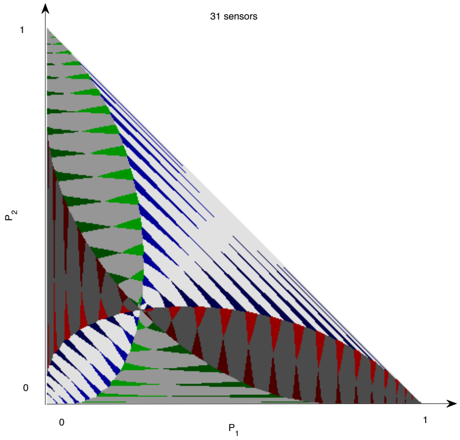

Figure: Areas that the NQS with one different LRQ outperforms the best IQS. The implications of different colors are designated in (10). The number of sensors is 31.

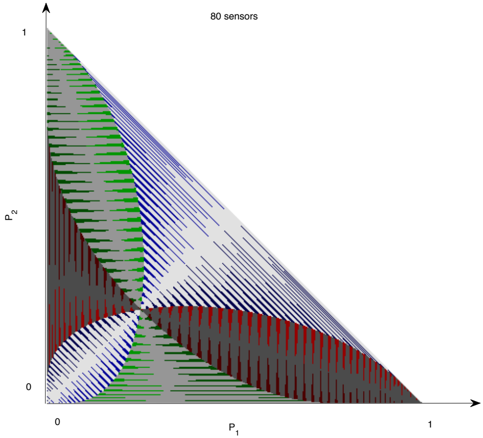

Figure: Areas that the NQS with one different LRQ outperforms the best IQS. The implications of different colors are designated in (10). The number of sensors is 80.

Conclusion and Future work

Conclusion

- We found via extensive trials that the optimal design is mostly identical but uses only few (one or two) different LRQs.
- By deriving the exact error formulas, we did locate a few line regions that the NQS outperforms the best IQS.

Future Work

- In fact, the technique we used should be able to extend to identify a region that the NQS outperforms the best IQS, but we defer this task as a future work.

- The other future work is to check whether adopting two distinct LRQs, not just one, can further improve the detection error.